ISSN 2278-3091
Volume 9, No.1.5, 2020
International Journal of Advanced Trends in Computer Science and Engineering
Available Online at http://www.warse.org/IJATCSE/static/pdf/file/ijatcse2191.52020.pdf
https://doi.org/10.30534/ijatcse/2020/2191.52020

Dielectric Properties of WC / Al_2O_3 Ceramic Composite in the X and Ku Bands

Ouhassan Youssef [1], Bri Seddik [2], Habibi Mohamed [1]
[1]Laboratory of Electronic Systems, Information Processing, Mechanics and Energy, Faculty of Sciences, Ibn Tofail University, Morocco
ouhassan.youssef@gmail.com, mohamed.habibi@hotmail.com
[2]Materials and Instrumentations group, Superior School of Technology, Moulay Ismail University, Morocco
briseddik@gmail.com

ABSTRACT
In this paper, we studied the effect of tungsten carbide (WC) content on the dielectric properties of WC/Al_2O_3 composite containing 20%, 30% and 40% by volume of WC. The results show that the permittivity of the WC/Al_2O_3 composite increases progressively with increasing WC content and decreases slightly with increasing frequency in both X and Ku band. Composites reinforced with 40% by volume of WC have better dielectric properties than composites that are less reinforced. A good agreement between the results of numerical simulations and published measurements was obtained in the X-band.

Key words: Complex permittivity, dielectric composite, effective permittivity, finite element method, transmission / reflection (T/R), WC, X-band, Ku-band.

1. INTRODUCTION

With the rapid development of radar detection and wireless communication around the world, many types of pollutants can affect the environment [1]. Therefore, materials absorbing electromagnetic waves have attracted much interest of researchers, due to the increase in electromagnetic pollution, which caused by the electromagnetic radiation and electromagnetic interferences [2].

Alumina (Al_2O_3) matrix ceramic composites play an important role in many applications and industries [3]. Tungsten carbide (WC) is a chemical compound with a high melting point of about 2870 °C and a boiling point of about 6000°C[4] .Its thermal conductivity is 110$W \cdot m^{-1} \cdot K^{-1}$ and thermal expansion coefficient 5.5 $\mu m \cdot m^{-1}.K^{-1}$ [4] . Because of its high electrical conductivity, tungsten carbide has been combined with alumina to form a new composite coating called WC/Al_2O_3 [4]. This composite has excellent electromagnetic wave-absorbing properties and has been added to radar-absorbing materials (RAM) [4] for use in aircraft, missiles and warships, where radiation resistance is both necessary and critical [5]. The recent development of RAMs with high absorption is of crucial importance in electronic equipment, mobile communications, military applications [6], and to solve the problems of reducing the objects radar visibility[7]. However, designing effective RAM requires precise knowledge of complex permittivity [6]. In the literature, several techniques have been proposed for determining the complex permittivity of materials; some are single frequency, while others offer broadband characterization [8].

In the present work, we adopt the method of transmission/reflection (T/R) based on rectangular waveguides. This technique offers characterization over a wide frequency range from 8.2GHz to 18GHz. The main objective is to study the effect of WC reinforcements on the dielectric properties of WC/Al_2O_3 composites, when the composition of the WC content varies from 20% to 40% by volume in the Al_2O_3 alumina matrix. Additionally, the determination of the complex permittivity of the WC/Al_2O_3 composites in the two frequency bands X and Ku. We use a program in MATLAB to calculate the complex permittivity from the transmission and reflection coefficients, extracted by the electromagnetic numerical simulation software.

2. THEORIES AND METHODS

In the microwave domain, the transmission/reflection (T/R) technique [9] has been used to characterize a dielectric material. This technique consists of placing the sample of material under test (MUT) inside the rectangular waveguide and calculating the parameters S_{ij}. We consider that only the dominant fundamental mode (TE_{10}) propagates inside the waveguide and the sample is precisely adjusted in a sample port. Figure 1 presents the simulation setup at X band.

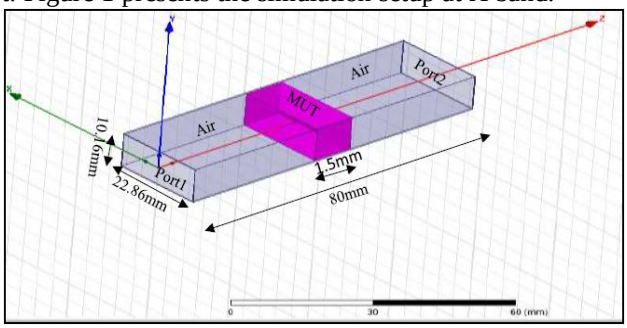

Figure 1: Schematic figure of the rectangular waveguide setup used for extraction of the material parameters in the X band.

In our study, we propose a mathematical approach based on the cascaded wave matrix [10]. This approach takes into account all the reflections of the electromagnetic wave on both sides of the sample through the waveguide[10].The technique mathematically eliminates output errors from the calculation cell [10]. Two measurements in T/R are sufficient to evaluate the complex permittivity of the dielectric sample: the first that the sample holder is filled with the reference dielectric material (Teflon), and the second with the material under test (MUT) [10]. We calculate the transmission matrices M_n according to [11]-[12]:

$$M_n = \frac{1}{S_{21n}}\begin{pmatrix} -\Delta & S_{11n} \\ -S_{22} & 1 \end{pmatrix} \quad (1)$$

with $\Delta = S_{11n}S_{22n} - S_{12n}S_{21n}$ and n = a or b

The corresponding transmission matrices M_a and M_b are calculated from the equation (1).

M_a: corresponds to the compute cell, which is empty or partially filled by a dielectric whose complex permittivity is known with precision on the frequency band studied.

M_b: corresponds to the compute cell partially filled by the sample to be characterised as the material under test(MUT).

The matrices M_a and M_b can also be written as a product of five matrices, as follows:

$$\begin{cases} M_a = x.T_{ref_a}.T_a.T_{ref_a}^{-1}.y \\ M_b = x.T_{ref_b}.T_b.T_{ref_b}^{-1}.y \end{cases} \quad (2)$$

Where:

• x and y are the error matrices assumed to be unchanged during the two calculations.

• T_{ref_n} is the transmission matrix corresponding to the impedance jump at the Air/Material interface (Air / sample / Air) causing reflections of the electromagnetic wave, including the transmission matrix.

$$T_{ref_n} = \frac{1}{1-\Gamma_n}\begin{pmatrix} 1 & \Gamma_n \\ \Gamma_n & 1 \end{pmatrix} \quad (3)$$

$$\Gamma_n = \frac{1-\frac{\gamma_n}{\gamma_0}}{1+\frac{\gamma_n}{\gamma_0}} \quad (\mu^*_r = 1) \quad (4)$$

$$T_n = \begin{pmatrix} T_d & 0 \\ 0 & \frac{1}{T_d} \end{pmatrix} \text{ with } T_d = e^{-\gamma_n d} \text{ and n=a or b} \quad (5)$$

Γ_n: the reflection coefficient at the Air Material interface.

T_n: the transmission matrix of a line of length d.

Or: $\gamma_0 = j\frac{2\pi}{\lambda_0}\sqrt{1-\left(\frac{\lambda 0}{\lambda c}\right)^2}$ (6)

And $\gamma_n = j\frac{2\pi}{\lambda_0}\sqrt{\varepsilon^*_{rn}\,\mu^*_{rn} - \left(\frac{\lambda_0}{\lambda_c}\right)^2}$ (7)

With $n = a$ or b

γ_0 and γ_n : the propagation constants in the air and in the dielectric respectively.

λ_c and λ_0 :the cut-off wavelength of the rectangular waveguide and the free space wavelength respectively.

ε^*_{ra} and ε^*_{rb} are the complex permittivity of the reference samples(Teflon) and MUT samples, respectively.

The matrix product $M_aM_b^{-1}$ eliminates the influence of the two error ports on the device parameters as shown in Equation(8):

$$M_aM_b^{-1} = x.T_{ref_a}.T_a.T_{ref_a}^{-1}.T_{ref_b}.T_b^{-1}.T_{ref_b}^{-1}.x^{-1} \quad (8)$$

Where M^{-1} means the inverse of the square matrix M.

Furthermore,equation (8) shows that $M_aM_b^{-1}$ and $T_{ref_a}.T_a.T_{ref_a}^{-1}.T_{ref_b}.T_b^{-1}.T_{ref_b}^{-1}$ are similar, and have the same trace defined by the sum of the diagonal elements.

$$Tr(M_aM_b^{-1}) = Tr(T_{ref_a}.T_a.T_{ref_a}^{-1}.T_{ref_b}.T_b^{-1}.T_{ref_b}^{-1}) \quad (9)$$

With Tr (M) is the trace of the square matrix (M).

The relation (9) is a nonlinear equation whose only unknown is the permittivity complex ε^*_{rb} of the material under test, such that:

$$f(\varepsilon_{rb}^*) = Tr(T_{ref_a}.T_a.T_{ref_a}^{-1}.T_{ref_b}.T_b^{-1}.T_{ref_b}^{-1}) \quad (10)$$

Note that *f* is a function of ε^*_{ra} , λ_0 , λ_c and d where ε^*_{rb} is the single unknown. Many complex values of ε^*_{rb} can satisfy the function *f*. If a good initial value of ε^*_{rb} is available, the resolution function *f* iteratively leads directly to the true value of ε^*_{rb}. This technique based on the cascade wave matrix (WCM) makes it possible to mathematically eliminate the matrices of errors x and y and to extract a nonlinear equation whose resolution can be done in an iterative manner via an algorithm of resolution. Equation (9) can be simplified if the air is taken as the reference dielectric

during the first compute, then: $\varepsilon_{ra}* = 1$, $\gamma_a = \gamma_0$ and $\Gamma_a = 0$. Equation (9) then becomes:

$$Tr(M_a M_b^{-1}) = Tr(T_a . T_{ref_b} . T_b^{-1} . T_{ref_b}^{-1}) = 2\frac{\Gamma_b^2 \cosh(\Lambda_a) - \cosh(\Lambda_b)}{\Gamma_b^2 - 1} \quad (11)$$

Or: $\Lambda_a = (\gamma_0 + \gamma_2)d$ and $\Lambda_b = (\gamma_0 - \gamma_2)d$

3 .RESULTS AND DISCUSSION

First, we study the effective permittivity of the WC / Al_2O_3 composite material as a function of the WC content for three permittivity contrasts between the spherical inclusions and the matrix . The results were obtained by simulations of the unit cell of the composite material in a three dimensional 3D using electromagnetic simulation software. We have performed simulations for an alumina dielectric matrix of permittivity ε_1 = 9.5 and the spherical inclusions of relative permittivity ε_2 for three contrastes $K = \frac{\varepsilon_2}{\varepsilon_1} = \frac{38}{9.5}, \frac{190}{9.5} and \frac{570}{9.5}$ .This contrasts were analysed by changing the volume fraction *f* of the spherical inclusions of radius R = 50 µm incorporated in the matrix from 0.8% to 80%.The inclusions are in permanent contact without any overlap. In all simulations, the phases are initially discharged and no longer contain free charges. The external electric field is applied in the direction (Oz).

Figure 2 shows the variation of the effective dielectric permittivity of the WC / Al_2O_3 composite as a function of the volume fraction of WC inclusions for three contrasts of permittivity K. The results of the simulations are compared with the classic Maxwell-Garnett mixing law.

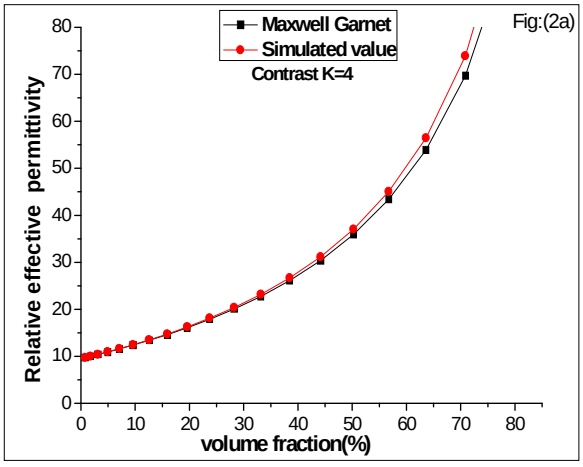

Figure (2a): For contrast K=4

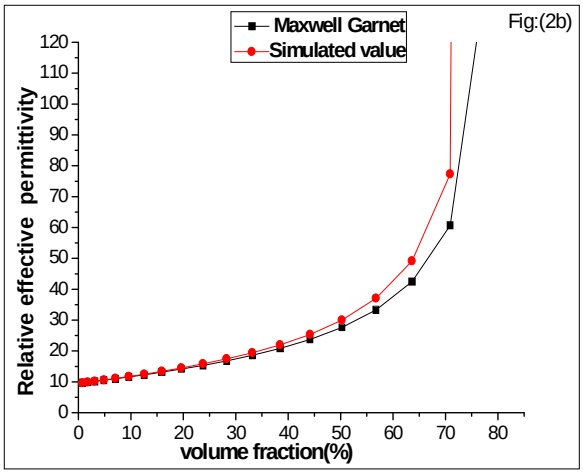

Figure (2b): For contrast K=20

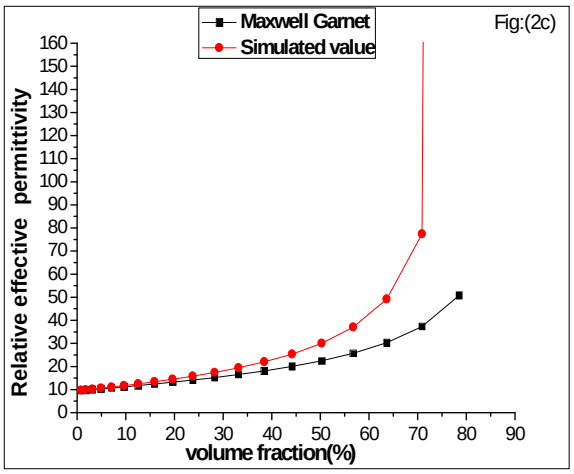

Figure (2c): For contrast K=60

Figure 2: Evolution of the effective permittivity of the WC / Al_2O_3 composite as a function of the WC content for three contrasts.

The results show that the effective permittivity of the composite studied depends on the WC content and on the permittivity contrast between the inclusions and the matrix. This permittivity increases with the content of WC in the matrix of Al_2O_3 alumina and of contrast K. This is explained by the fact that when the filling rate increases, the distance between spherical inclusions decreases and the percolation threshold of the composite material decreases, which means that the material conductivity is improved [13]. Therefore, the effective permittivity increases. The comparison between the results of simulations with the Maxwell-Garnett law indicates that this law is more suitable for predicting with more precision the effective permittivity of the composite over the entire range studied for low contrasts K≤4. For contrasts K≥4, on the one hand, the simulated permittivity is acceptable if the mixture is diluted up to 30% of the volume fraction. On the other hand, Maxwell-Garnett's law is unable to estimate the effective permittivity in high concentration of inclusions

greater than 30% of the volume fraction and for high contrasts. This observed diverging behaviour is mainly due to the interactions between the inclusions, which become very significant at high concentrations [14].

To characterize the composite WC/Al_2O_3 in both X and Ku bands, we used the Transmission/Reflection technique (T/R). The dielectric material sample WC/Al_2O_3 has the dimensions (22.86mm*10.16mm*1.5mm) in X-band (figure1) and (15.8mm*7.9mm*1.5mm) in Ku-band. This sample is well adjusted in a rectangular waveguide, in order to measure the S_{ij} parameters. The application of the transmission/reflection technique makes it possible to calculate the complex permittivity of the composite WC/Al_2O_3 from reflection coefficient S_{11} and transmission coefficient S_{21}. we simulate the cell presented in figure 1. by the electromagnetic numerical simulation software.

Figures 3 and 4 represent respectively the frequency evolution of the real ε´ and imaginary ε´´ part of the complex relative permittivity, for the three WC contents of the ceramic composite material WC/Al_2O_3 in the X and Ku bands.

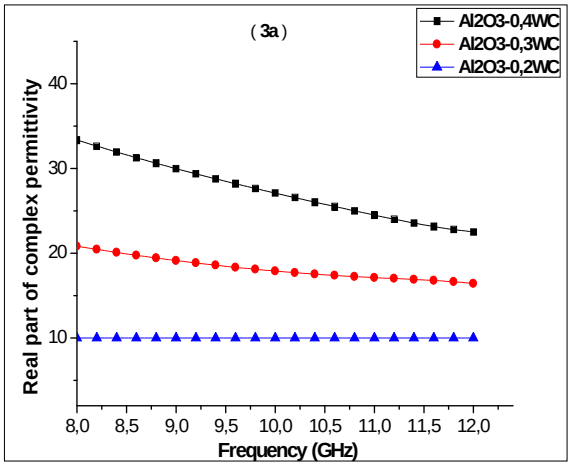

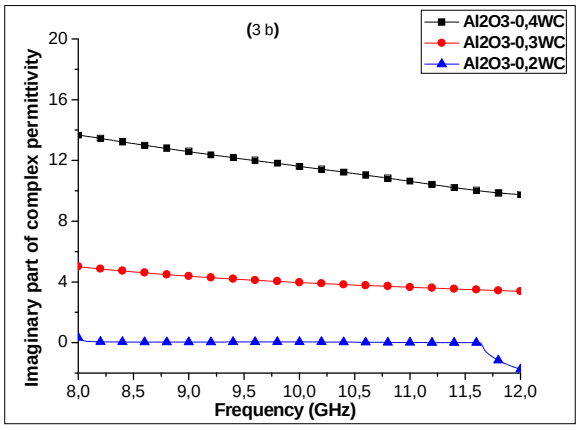

Figure 3: The permittivity of Al_2O_3/WC composites (3a) Real part of permittivity (ε'); (3b) Imaginary part of permittivity (ε") in the X band.

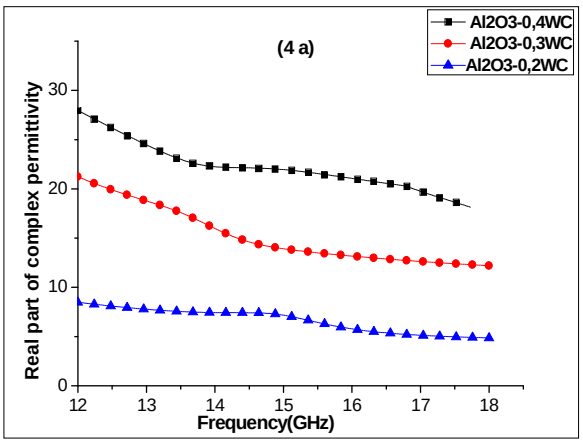

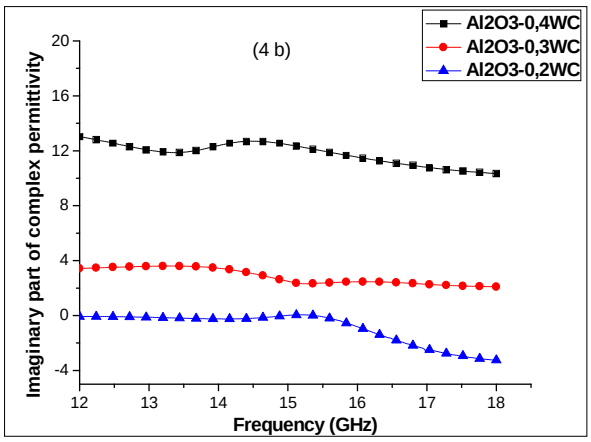

Figure 4: The permittivity of Al_2O_3/WC composites (4a) Real part of permittivity (ε'); (4b) Imaginary part of permittivity (ε") in the Ku-band.

The results show that the values of the real ε´ and imaginary ε´´ parts of the complex permittivity are generally high for the composite with 40% WC content. Because WC tungsten carbide is a conductive ceramic with excellent conductivity, while Al_2O_3 alumina is a non-conductive material [4]. When the WC and Al_2O_3 materials are mixed and transformed into a composite, the WC inclusions are dispersed in the dielectric matrix and quantities of interfaces are formed between these different materials. If the composite subjected to an alternating electromagnetic field, moving charges are trapped and accumulate at the interfaces, resulting in interfacial polarization [15]. As the WC content increases, more charges mobile are produced at the interfaces, resulting in improved electronic polarization and relaxation polarization. Therefore, the real part of the permittivity increases with increasing WC content. In the microwave frequency range, the imaginary part of the permittivity ε´´ is determined by both polarization relaxation loss and conduction loss [13].If the WC content increases, the conductivity increases significantly, resulting in increased conduction loss. As well as the relaxation polarization is reinforced, which leads to an increase in the corresponding relaxation loss. Therefore, improving the imaginary part of

the complex permittivity. For these ceramic composites, the real ε' and imaginary ε'' parts decrease slightly with increasing frequency. Because the alumina Al_2O_3 generally has a poor conductivity and the dielectric constant is mainly produced by the electric dipole. When it forms a mixture with WC tungsten carbide, the dielectric constant of the mixture is mainly dependent on three factors: interface, space charge and electrical dipole polarization [16]-[17]. These three factors are mainly correlated with frequency, namely that they decrease progressively with increasing frequency and therefore the dielectric constant also decreases with increasing frequency. The values of the imaginary part probably remains constant for the composite with 20% in WC content. This indicates the existence of low dielectric losses for the low WC content.

Tables 1 and 2 present respectively the values of the real and imaginary parts of the dielectric permittivity simulated and obtained by measurements in the literature [4] for the composites studied. These values are taken at selected points of the frequency across the X band. The precision of the variation of the results obtained can be determined by calculating the relative error $\%Error = \left|\frac{\varepsilon_s - \varepsilon_m}{\varepsilon_m}\right| \times 100$ compared to the measurement results in the literature [4].

Table 1: Simulated, measured values and the relative error compared to the measured values of the real part of the dielectric permittivity for selected points of the frequency in the X band.

Frequency (GHz)	**Al_2O_3-0.2WC**			**Al_2O_3-0.3WC**			**Al_2O_3-0.4WC**		
	ε'_s Calculated	ε'_m Literature	Error $\frac{\Delta\varepsilon'}{\varepsilon'_m}$ (%)	ε'_s Calculated	ε'_m Literature	Error $\frac{\Delta\varepsilon'}{\varepsilon'_m}$ (%)	ε'_s Calculated	ε'_m Literature	Error $\frac{\Delta\varepsilon'}{\varepsilon'_m}$ (%)
9	10.02	9.85	1.72	19.16	19.72	2.83	32	33	3.03
10	9.98	9.78	2.04	18.56	19.70	5.78	30	32	6.25
11	9.97	9.76	2.15	18.20	19.69	7.56	28	31	9.67

Table 2: Simulated, measured values and the relative error compared to the measured values of the imaginary part of the dielectric permittivity for selected points of the frequency in the X band.

Frequency (GHz)	**Al_2O_3-0.2WC**			**Al_2O_3-0.3WC**			**Al_2O_3-0.4WC**		
	ε''_s Calculated	ε''_m Literature	Error $\frac{\Delta\varepsilon''}{\varepsilon''_m}$ (%)	ε''_s Calculated	ε''_m Literature	Error $\frac{\Delta\varepsilon''}{\varepsilon''_m}$ (%)	ε''_s Calculated	ε''_m Literature	Error $\frac{\Delta\varepsilon''}{\varepsilon''_m}$ (%)
9	0.44	0.45	2.22	5.52	5.35	3.17	12.10	12.70	4.72
10	0.34	0.35	2.85	4.96	5.33	6.94	11.54	12.50	7.68
11	0.33	0.34	2.94	4.84	5.30	8.68	10.60	12	11.66

The histograms in Figure 5 illustrate the percentages of the errors between the simulated and measured values of the real part and the imaginary part of the relative dielectric permittivity at these points.

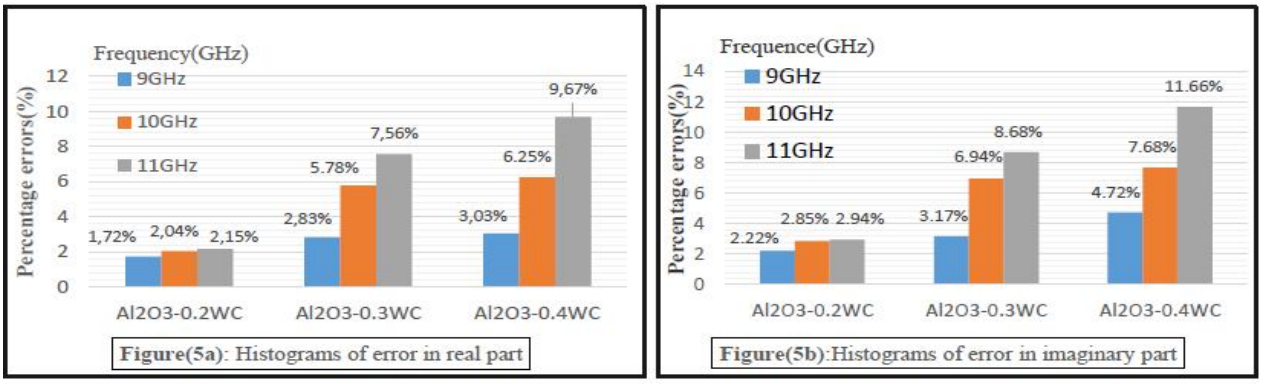

Figure 5: Histograms of the percentage errors between simulated and measured values (literature) of the complex dielectric permittivity for selected points in the X-band frequency range. Figure (5a): % error in the real part and Figure (5b): % error in the imaginary part.

From the histograms in Figure 5. On the one hand, we found that the percentage of errors between the values of numerical simulations and those obtained in the literature by measurement is low for the composite Al_2O_3-0.2WC and for the low frequencies. On the other hand, we find that this percentage is important in the imaginary part in comparison with the real part; its value for the imaginary part can reach 11.66% for the composite Al_2O_3-0.4WC at the frequency 11 GHz. However, this percentage for the real part is less than 1.75% for the same composite at 9GHz. The results obtained in this work are in agreement with the results published [4], with errors observed in the previous histograms. In general, simulation and measurement describe a similar dielectric behaviour for the materials studied.

4. CONCLUSION

In this study, we used the transmission / reflection method (T/R) to determine the complex permittivity of the WC/Al_2O_3 composite. We also employed the finite element method to predict the permittivity of this composite. The Maxwell-Garnett theory made it possible to predict the effective permittivity of the material studied for low volume fractions and low contrast. We found that the values of the real and imaginary parts of the complex permittivity increase with the content of WC. These values decreased as the frequency increased in both the X and Ku bands. The percentage of error calculated shows good agreement between the results obtained and published in the X-band. The composites studied seem to be very good candidates for the anti-reflection of coating materials by absorption of microwaves

REFERENCES

1. H.M. Shehata, D.A. Ali, I.M. Al-Akraa, H.A. Elazab, and H.A. Elsawy. **Development of Novel adsorbent for Industrial waste water treatment**, IJATCSE, vol.9, No.1, pp.704-712, January-February 2020.
2. S.F.Jainal, and C. C. Kang. **Electromagnetic Interference in the Railway Spot Communication Systems,** IJATCSE, vol.9, No.1.1, pp.114-118, 2020.
3. S.N. Grigoriev, M.A. Volosova, P.Y.Peretyagin, A.E. Seleznev, A.A. Okunkova, and A.Smirnov. **The effect of TiC additives on mechanical and electrical properties of Al_2O_3 ceramic**, Applied Sciences (Switzerland), vol.8, No.12,Article number 2385, November 2018.
4. T.Shao, H.Ma, M. Feng, J.Wang, M.Yan , JF.Wang, S. Zhao and S.Qu . **A thin dielectric ceramic coating with good absorbing properties composed by tungsten carbide and alumina**, Journal of Alloys and Compounds, Vol. 818, Article number 152851, March 2020.
5. M. S. Pinho, M. L. Gregori, C. R. Nunes, and B. G. Soares. **Performance of Radar Absorbing Materials by waveguide measurements for X and Ku band frequencies**, J. Eur. Polym,vol. 38, pp. 2321-2327, November 2002.
6. N.Jebbor, S.Bri, and M. C. Elboubakraoui. **Effective Complex Permittivity Determination and Microwave Absorption Properties of a Granular Dielectric Composite Material**, Procedia Computer Science, Vol. 151, pp. 1022-1027, May 2019.
7. S.Vitalii, V.Oleh, T.Oksana, P.Olha, S.German, T.Maksym, Z.Viktor, and K.Marianna. **Influence of the Composite Materials Nonlinear Properties with Radioisotope Inclusions on Reflected Radiation**, IJATCSE, vol.8, No.6, pp.2716-2720, November 2019.
8. M. C. Elboubakraoui, S. Bri, and J. Foshi. **Electromagnetic Properties of Composites CoFeNiBSiMo, CoFeBSiCr and CoMnSiB in wide frequency bande**, Materials Science and Engineering, Vol. 186, No.1, Article number 012012, March 2017.

9. X. Zhao, Y. Wu, Z.Fan, and F.Li. **Threedimensional simulations of the complex dielectric properties of random composites by finite element method**, J. Appl. Phys, Vol. 95 , No. 12, pp. 8110-8117, June 2004.
10. N. Jebbor, S. Bri, A.M. Sánchez,and M.Chaibi . **Afast calibration-independent method for complex permittivity determination at microwave frequencies**, Measurement, Vol. 46, pp. 2206-2209, April 2013.
11. U.C.Hasar and O. Simsek. **On the application of microwave calibration-independent measurements for noninvasive thickness evaluation of medium- or low-loss solid materials**, Prog. Electromag. Res., Vol. 91, pp. 377-392, 2009.
12. U.C.Hasar. **Determination of full S-parameters of a low-loss two-port device from uncalibrated measurements**, review of scientific instruments, Vol .89, No.12, 124701, 2018.
13. Y. Wang, F .Lou, W.C. Zhou, and D.M. Zhu. **Dielectric and Microwave Absorption Properties of TiC-Al_2O_3/Silica Coatings at High Temperature**, Journal of electronic materials, Vol. 46, No. 8, 2017.
14. M. C. Elboubakraoui, S. Bri, and J.Foshi. **Dielectric Properties of SiCf/SiC Composites**, FME Transactions, Vol. 46, 86-92, February 2018.
15. Y. Qing, W. Zhou, F. Luo, and D. Zhu. **Titanium carbide (MXene) nanosheets as promising microwave absorbers**, Journal of Ceramics International, Vol. 42, pp. 16412-16416, November 2016.
16. G. M. Tsangaris, G. C. Psarras, and N. Kouloumbi. **Electric modulus and interfacial polarization in composite polymeric systems**, Journal of Materials Science 33, pp. 2027-2037, April 1998.
17. N. Bogris, J. Grammatikakis, and A. N. Papathanassiou. **Dipole and interfacial polarization phenomena in natural single-crystal calcite studied by the thermally stimulated depolarization currents method**, Phy. Rev. B, Vol. 58, No. 16, October 1998.